ChemComm

Accepted Manuscript

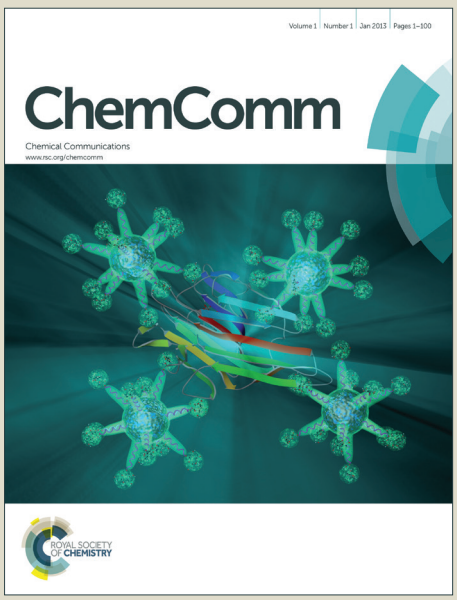

ROYAL SOCIETY OF CHEMISTRY

www.rsc.org/chemcomm

Cite this: DOI: 10.1039/c0xx00000x

www.rsc.org/xxxxxx

ARTICLE TYPE

Electrochemical Synthesis of Luminescent MoS_2 Quantum Dots†

Deepesh Gopalakrishnan,[a‡] Dijo Damien,[a‡] Bo Li,[b] Hemtej Gullappalli,[b] Vijayamohanan K. Pillai,[c] Pulickel M. Ajayan[b] and Manikoth M. Shaijumon[*a]

Received (in XXX, XXX) Xth XXXXXXXXX 20XX, Accepted Xth XXXXXXXXX 20XX

DOI: 10.1039/b000000x

Size-controlled synthesis of luminescent quantum dots of MoS_2 (≤ 2 layers) with a narrow size distribution, ranging from 2.5 to 6 nm, from their bulk material, using a unique electrochemical etching of bulk MoS_2, is demonstrated. Excitation-dependent photoluminescence emission is observed in the MoS_2 QDs. "As synthesized" MoS_2 QDs also exhibit excellent electrocatalytic activity towards hydrogen evolution reaction.

Graphene and graphene-related materials have been intensively studied in recent times and wide attention has been given to exploit their unique electrical and optical properties to realize graphene-based devices. However, the semi-metallic nature of pristine graphene limits its use in nanoelectronics/photonics. Various approaches to introduce band gap in graphene have been attempted, such as cutting into nanoribbons,[1-3] introducing defects,[4] making quantum dots[5] with limited success. Recent advances in 2-dimensional (2D) layered materials beyond graphene have opened up a new horizon for a novel class of low-dimensional systems with its extra-ordinary properties for applications in electronics, optoelectronics, energy conversion and storage.[6,7] Interesting physical and chemical properties exhibited by these materials along with its potential applications, upon thinning down to single or few layers, have driven lot of attention in recent times. As the bulk MoS_2 has an indirect band gap of 1.2 eV, it does not show photoluminescence properties; however, as the thickness of this material comes down to monolayer, electronic properties changes drastically resulting in a direct band gap semiconductor with a band gap of 1.9 eV.[8] More recently, single/few layered nanostructures of MoS_2 has attracted significant attention amongst other members of the transition metal dichalcogenides (TMDCs) family, such as WS_2, $MoSe_2$, WSe_2, etc. [9,10]

Several recent reports have demonstrated MoS_2 based electronic devices with improved performances compared to graphene based ones.[11-13] For ultra-thin MoS_2 nanosheets, when confined to zero-dimension (0D), the quantum size effects[14] and the edge effects[15] become very significant, resulting in interesting physical properties. However, studies on MoS_2 quantum dots have been less explored, particularly in terms of novel synthetic strategies developed to achieve accurate size control. Previously reported methods are tedious and/or yielding poly-dispersed distribution of particles. [16, 17] With a similar 2D layered structure of graphite and MoS_2, held together by common van der Waals forces, the exfoliation techniques established for graphene quantum dots (GQDs), from its 2D nanosheets viz. hydrothermal cutting,[18] sonication[19]etc., have been successfully extended for the preparation of MoS_2 QDs. For instance, inverse micellar cages have been successfully employed for the size tunable-uniform synthesis of MoS_2 quantum dots[14] and GQDs.[20] However, several of these techniques are time consuming and involve harsh conditions, resulting in QDs with low yield and a large size distribution. In contrast, the electrochemical strategy developed for the synthesis of graphene nanoribbons/nanosheets and GQDs from bulk graphite, graphene sheets and multiwalled nanotubes (MWNTs) has been shown to be remarkably effective with several advantages viz. cost effective, ecofriendly, fast, etc., compared to other techniques.[3, 21-24]Using a similar approach, recent reports have demonstrated the exfoliation of thin MoS_2 nanosheets from their bulk crystal with reasonable yields.[25,26] However, several of these studies follow tedious multi-step processes to obtain MoS_2 layers and QDs.[23] Size controlled synthesis of MoS_2 QDS still remains a challenge.

Herein we report, for the first time, a single-step electrochemical approach for the synthesis of luminescent QDs of MoS_2, from its bulk material, in aqueous ionic liquid solutions of 1-Butyl-3-methylimidazolium Chloride, ([BMIm]Cl) and Lithium bis-trifluoromethylsulphonylimide (LiTFSI). A good control on the size distribution of MoS_2 QDs has been achieved by varying the applied DC voltage and the composition of the electrolyte. The resultant QDs exhibited excitation dependent-luminescence, quite similar to that observed for both carbon and silicon nanoparticles.[27] In addition, we demonstrate excellent electrocatalytic activity of these materials for Hydrogen evolution reaction (HER). The electrochemically driven process by the generation of oxygen and hydroxyl free radicals, involving environmentally benign ionic liquids, is efficient, economical and fast, to synthesize MoS_2 QDs for its emerging applications in quantum information systems, nanoelectronics and energy conversion technologies.

Fast growth of MoS_2 QDs with varying sizes were achieved by applying a constant DC potential of 5 V across bulk MoS_2 pellets in a two-electrode cell (1 cm in diameter, kept 1 cm apart; Supporting Information, Fig. S1.) in different concentrations (0.1, 1 and 5 wt.%) of aq. LiTFSI or [BMIm]Cl. TEM images of electrochemically exfoliated MoS_2 QDs obtained with varying electrolyte compositions show a uniform size distribution (Fig. 1). More significantly, the use of a LiTFSI based aq. electrolyte

with concentration of 0.1 and 1 wt.% yields particles with lateral size of 2.5 and 4.6 nm respectively (Fig. 1A,B), whereas, QDs of slightly larger sizes, 2.8 and 5.8 nm, are obtained using [BMIm]Cl based aq. electrolytes at 0.1 and 1 wt.% concentrations, respectively (Fig. 1C,D).

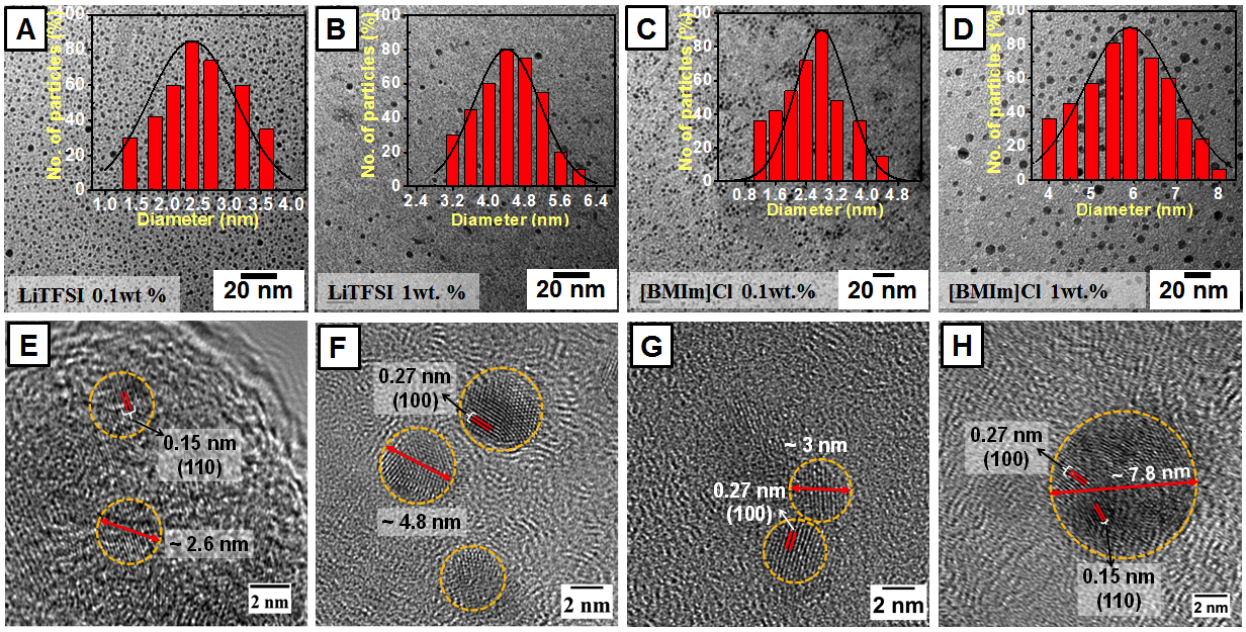

Fig. 1 Electron microscopic characterization of electrochemically exfoliated MoS_2 QDs obtained at an applied potential of 5 V. (A, B) TEM images of MoS_2 QDs synthesized using aq. LiTFSI electrolyte with 0.1 and 1.0 wt% concentration, respectively. The corresponding HRTEM images (E and F), respectively, show average particle size of 2.5 nm and 4.6 nm. Aq. [BMIm]Cl based electrolyte lead to the formation of slightly larger particles of dimension 2.8 nm and 5.8 nm with concentrations of 0.1 and 1.0 wt% respectively, as shown in the TEM (C, D) and HRTEM images (G, H).

The high resolution TEM images of MoS_2 QDs obtained using LiTFSI (Fig. 1E, F) and [BMIm]Cl (Fig. 1G, H) based aq. electrolytes show the corresponding lattice spacing consistent with the reported values (ICDD- PDF#: 00-006-0097). However, the variation in the electrolyte composition did not affect the thickness of the MoS_2 QDs obtained as evident from the atomic force microscopy (AFM) analysis (Fig. S2, S3, ESI†). Thickness of the particles corresponds to mono/bi layered MoS_2. Fig. S2A and S2B, respectively, show the AFM image and corresponding height profile of MoS_2 QDs synthesized using aq. [BMIm]Cl electrolyte of concentration 0.1 wt%. Thickness of the MoS_2 QDs obtained was measured to be ~ 0.8 -1.5 nm, which is slightly higher than the theoretical value for monolayer (0.64 nm) or bilayer MoS_2.[28] This could be due to swelling of the layers by the incorporation of electrolyte ions. Fig. S2C, S2D, respectively, show the AFM images and corresponding height profile of the MoS_2 QDs formed using 1 wt.% concentration of [BMIm]Cl. A similar trend is also observed in MoS_2 QDs synthesized using aq. LiTFSI with a concentration of 0.1 wt.% and 1 wt.% as well, as shown in Fig. S3. The corresponding height profiles confirm mono/bi-layered MoS_2 clusters (Fig.S3 B, D, ESI†). Very dilute aqueous electrolytes and pelletized MoS_2 electrodes employed in the present work make the whole approach cost-effective and eco-friendly, compared to the use of bulk MoS_2 crystals.[25]

The mechanism for the synthesis of MoS_2 QDs with single/few layers, could be easily understood from the generation of free radicals that trigger the initial cleavage leading to further exfoliation of the bulk material, similar to that observed during the electrochemically driven synthesis of graphene QDs or nanoribbons.[3, 21] With very dilute aq. electrolyte, exotic hydroxyl and oxygen free radicals are formed under the applied DC potential, which is higher than the electrochemical window of the electrolyte. As time progresses, MoS_2 anode swells by the incorporation of $TFSI^-$ and Cl^{3-} anions respectively in LiTFSI and [BMIm]Cl based electrolytes and MoS_2 QDs start dissolving in the electrolyte, as depicted schematically in Fig. S4. This dissolution coarsens the surface of bulk MoS_2 pellet (anode) as evidenced from SEM images (Fig. S5, ESI†). Interestingly, this process leads to slight oxidation of Mo and S edges in the as-formed QDs as further confirmed from the XPS analysis (Fig. S6, ESI†). Mo signal shows broad bands corresponding to binding energies centered ~232 and 235 eV indicating the presence of mixed valences of +4 and +5. Pristine MoS_2 exhibits Mo3d5/2, Mo3d3/2 and S2p3/2 binding energies at 229.4, 232.5 and 162.2 eV respectively.[29] The observed peak at 168 eV correspond to the presence of S-O bonds,[30] which could have resulted from partial oxidation of MoS_2 in presence of aq. electrolyte under the applied DC potential. The XPS results obtained for MoS_2 QDs synthesized using both electrolytes were similar. Though such oxidation might slightly alter the electronic properties of pristine MoS_2,[31, 32] this could lead to generation of active surface sites with high reactivity towards better hydrogen evolution reaction (HER).[33]

In order to further confirm the presence of MoS_2 QDs, absorption spectra were recorded for the exfoliated samples (Fig. 2A). An absorption shoulder band centered on 370 nm was observed which corresponds to the excitonic feature of monodispersed MoS_2.[14,34,35]

Photoluminescence (PL) speactra have been recorded for the MoS_2 QDs and the obtained broad peak ~ 400 nm could be attri-

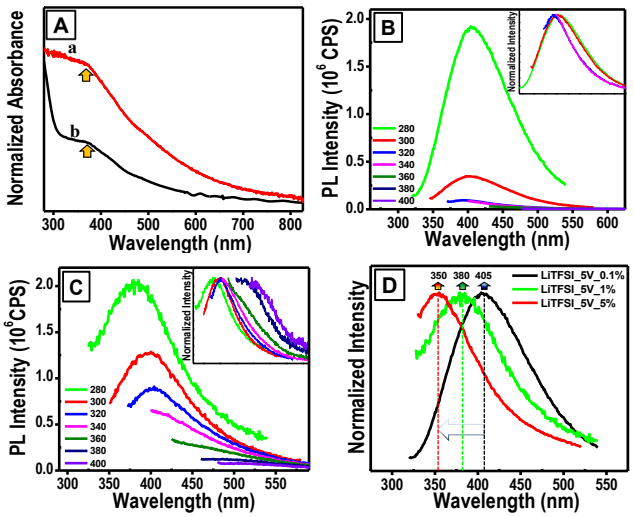

Fig.2 (A) UV-Vis absorption spectra of MoS_2 QDs formed using (a) [BMIm]Cl and (b) LiTFSI electrolytes. Photoluminescence spectra of MoS_2 QDs obtained with 0.1 wt% (B) and 1 wt% (C) of LiTFSI. Blue shift in the emission spectrum of MoS_2 QDs is observed as the electrolyte concentration is increased (D).

buted to direct band edge recombination.[36] Another interesting feature exhibited by the MoS_2 QDs is the excitation dependent photoluminescence emission (Fig. 2B-D), similar to that observed for GQDs,[24,27] solubilized carbon nanotubes[37] and suspended silicon nanocrystals.[38] However, the exact origin of excitation dependent photoluminescence of GQDs and similar species are still under debate.[39]Apart from the emission originating from the quantum sized MoS_2 core,[40] it may also arise from the charge transfer from the oxygen containing functional groups as in the case of GQDs.[19] For example, Pang and co-workers have studied the origin of luminescence in GQDs in detail and concluded that the surface states are the key to the luminescence of GQDs.[24, 41] A similar mechanism is operative here in the case of MoS_2 QDs as well. A low intensity and excitation dependent luminescence exhibited by the MoS_2 QDs in the present study imply the origin of photoluminescence from the exciton recombination at the electron (hole) trap constituted by uncompensated positive (negative) charge at the dangling bonds. As the salt to water ratio of the electrolyte increases, the particle size increases from 2.5 to 4.6 nm and 2.8 to 5.8 nm in aq. LiTFSI and aq. [BMIm]Cl respectively. As the size decreases a concomitant red shift in the luminescence emission from 350 to 380 nm and 375 to 400 nm in aq. LiTFSI (Fig.2B,C) and aq. [BMIm]Cl (Fig.S7A,B, ESI†), respectively, has been observed. Tuning of luminescence emission by systematically varying the electrolyte composition is further verified at a higher electrolyte concentration of 5 wt% as shown in Figure 2D. This was further investigated by time resolved emission spectroscopy obtained by time-correlated single photon counting technique. Accordingly, the time resolved photoluminescence spectra of MoS_2 QDs synthesized using 0.1 and 1.0 wt% aq. LiTFSI electrolytes (Fig. S8, ESI†) show three components which are relatively slow (ns time scale) compared to time constant for the direct excitonic recombination of monolayer MoS_2 nanosheets, which is of the order of picoseconds (disregarding the band gap widening due to the confinement effect).[42] As the particle size decreases the surface to volume ratio increases and the surface trap states due to the uncompensated sulfide ions and metal ions increases and thus results in the formation of deeper traps resulting in the red shifted photo emission.[43]As the applied potential increases, the exfoliation becomes more vigorous and QDs start dissolving at a faster rate. The blue shift in the photoluminescence emission spectrum with the increased salt to water ratio of the electrolyte is seen even at a higher applied potential as high as 10 V and at a concentration as high as 5 wt.% (Fig. S9, ESI†) supporting this faster dissolution mechanism.

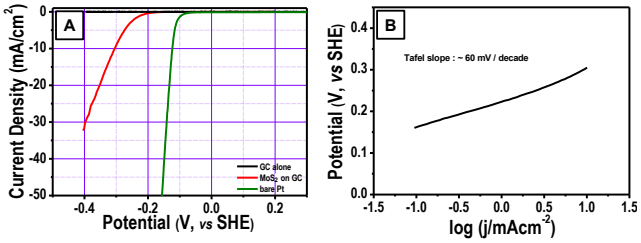

Fig.3 Electrocatalytic properties of MoS_2 QDs obtained using 1 wt% [BMIM]Cl electrolyte. (A) Polarization curves of the MoS_2 QDs, bare Glassy carbon and bare Pt electrodes obtained in 0.5 M H_2SO_4 at a scan rate of 2 mV/s. (B) Tafel plot obtained from the polarization curve show relatively small slope of 60 mV per decade.

The presence of active edge sites in MoS_2 nanosheets and QDs makes them attractive as an efficient electro catalyst for hydrogen evolution reaction (HER). To demonstrate the superior electrocatalytic properties of these nanostructures, we studied the electrochemical activity of MoS_2 QDs for HER in 0.5M H_2SO_4 solution using a typical three electrode system. MoS_2 QDs prepared using [BMIm]Cl based aq. electrolyte (1 wt.%), with an average particle size of 6 nm, drop casted on freshly polished glassy carbon electrode (GC) is taken as the working electrode. Platinum and Ag/AgCl were used as counter and reference electrodes respectively. The obtained polarization curve for MoS_2 QDs showed high catalytic activity, with an onset potential of ~210 mV vs. SHE (Fig.3A), which is comparable with the values reported in recent reports.[44, 45] The results are compared with bare GC and Pt electrodes, as shown in Fig.3A. The HER activity was further investigated through the Tafel plot, wherein the slope was found to be 60 mV per decade (Fig.3B) which suggests the presence of a large number of active catalytic edges resulting in improved reaction kinetics of the electrochemically exfoliated MoS_2 QDs. Another important HER rate parameter, namely the exchange current density, j_0, can be estimated by extrapolating the Tafel plot and was found to be 4.5 x 10^{-5} Acm^{-2}. The high exchange current density obtained also reflects the abundance in the number of active edge sites.[46] Thus, the relatively small Tafel slope along with a large exchange current density indicating improved HER activity, can be correlated with the presence of a large number of active edge sites in such ultra-small nanoparticles of MoS_2 along with their increased surface area.[34, 47, 48] The enhanced edge to basal plane ratio results in better electron transfer and easy access of active Mo edges for the adsorption of Hydrogen atom.[33, 48]

In summary, we have demonstrated a new approach for the controlled synthesis of luminescent QDs of MoS_2 with a narrow size distribution, from their bulk material, using an electrochemical etching process. MoS_2 QDs of very small lateral

sizes ranging from 2.5 to 6 nm and with single/few layer thickness were obtained using a very dilute aq. electrolyte solution. As-synthesized MoS_2 QDs showed excitation dependent luminescence, which could be further improved by surface passivation. MoS_2 QDs drop-casted on glassy carbon electrode showed excellent HER activity with an onset potential of ~210 mV and with a Tafel slope of 60 mV/decade. The presence of a large number of active edge sites in such ultra-small MoS_2 QDs would enable several new directions and opportunities in energy conversion technologies.

Notes and references

[a]*Indian Institute of Science Education and Research Thiruvananthapuram, CET Campus, Sreekaryam, Thiruvananthapuram, Kerala, 695 016, India. E-mail: shaiju@iisertvm.ac.in*
[b]*Department of Materials Science and Nano Engineering, Rice University, Houston, Texas, 77005, USA.*
[c]*CSIR-Central Electro Chemical Research Institute, Karaikudi, Karaikudi- Tamilnadu,630006, India.*

† Electronic Supplementary Information (ESI) available: [Experimental methods, experimental setup for the electrochemical exfoliation, SEM images, AFM images and height profiles, XPS spectra]. See DOI: 10.1039/b000000x/

‡ Deepesh Gopalakrishnan and Dijo Damien contributed equally. This work has been partially supported by the Board of Research in Nuclear Sciences (BRNS), Department of Atomic Energy (DAE), Govt. of India, through a DAE Young Scientist Research Award (No. 2012/20/34/5/BRNS). The authors thank Indo-US Science and Technology Forum (IUSSTF) for the Indo-US joint R&D network center [IUSSTF/JC/22-2012/2013-14]. D.D. acknowledges CSIR, Govt. of India, for the research fellowship. B.L. and P.M.A acknowledge the support from FAME, one of six centers of STARnet, a Semiconductor Research Corporation program sponsored by MARCO and DARPA.

1 L. Jiao, L. Zhang, X. Wang, G. Diankov and H. Dai, Nature, 2009, **458**, 877.
2 D. B. Shinde, J. Debgupta, A. Kushwaha, M. Aslam and V. K. Pillai, *J. Am. Chem. Soc*., 2011, **133**, 4168.
3 D. Damien, B. Babu, T. N. Narayanan, A. L. Reddy, P. M. Ajayan and M. M. Shaijumon, Graphene, 2013**, 1**, 37.
4 F. Banhart, J. Kotakoski and A. V. Krasheninnikov, *ACS Nano*, 2010, **5**, 26.
5 L. Li, G. Wu, G. Yang, J. Peng, J. Zhao and J.-J. Zhu, *Nanoscale*, 2013, **5**, 4015.
6 S. Z. Butler, S. M. Hollen, L. Cao, Y. Cui, J. A. Gupta, H. R. Gutiérrez, T. F. Heinz, S. S. Hong, J. Huang, A. F. Ismach, E. Johnston-Halperin, M. Kuno, V. V. Plashnitsa, R. D. Robinson, R. S. Ruoff, S. Salahuddin, J. Shan, L. Shi, M. G. Spencer, M. Terrones, W. Windl and J. E. Goldberger, *ACS Nano*, 2013, **7**, 2898.
7 R. Mas-Balleste, C. Gomez-Navarro, J. Gomez-Herrero and F. Zamora, *Nanoscale*, 2011, **3**, 20.
8 G. Eda, H. Yamaguchi, D. Voiry, T. Fujita, M. Chen and M. Chhowalla, *Nano Lett.*, 2011, **11**, 5111.
9 M. Chhowalla, H. S. Shin, G. Eda, L.-J. Li, K. P. Loh and H. Zhang, *Nat Chem*, 2013, **5**, 263.
10 X. Huang, Z. Zeng and H. Zhang, Chem Soc Rev, 2013, 42, 1934.
11 N. R. Pradhan, D. Rhodes, Q. Zhang, S. Talapatra, M. Terrones, P. M. Ajayan and L. Balicas, *Appl. Phys. Lett.,* 2013, **102,** 123105.
12 H. Wang, L. Yu, Y.-H. Lee, Y. Shi, A. Hsu, M. L. Chin, L.-J. Li, M. Dubey, J. Kong and T. Palacios, *Nano Lett.*, 2012, 12, 4674.
13 R. Ganatra and Q. Zhang, ACS Nano, 2014, **8**, 4074.
14 J. P. Wilcoxon and G. A. Samara, *Phys. Rev. B*, PRB, 1995, **51**, 7299.
15 S. Mathew, K. Gopinadhan, T. K. Chan, X. J. Yu, D. Zhan, L. Cao, A. Rusydi, M. B. H. Breese, S. Dhar, Z. X. Shen, T. Venkatesan and J. T. L. Thong, *Appl. Phys. Lett.*, 2012, **101,**102103.
16 Borrelli, N. F.; Luong, J. C. *SPIE* 1987, ***0866***, 104-109.
17 M. W. Peterson, M. T. Nenadovic, T. Rajh, R. Herak, O. I. Micic, J. P. Goral and A. J. Nozik, , *J. Phys. Chem*., 1988, **92**, 1400.
18 D. Pan, J. Zhang, Z. Li and M. Wu, *Adv. Mater*., 2010, **22**, 734.
19 J. Zhou, C. Booker, R. Li, X. Zhou, T.-K. Sham, X. Sun and Z. Ding, *J. Am. Chem. Soc*., 2007, **129**, 744.
20 W. Kwon and S.-W. Rhee, *Chem.Commun.*, 2012, **48**, 5256.
21 J. Lu, J.-x. Yang, J. Wang, A. Lim, S. Wang and K. P. Loh, *ACS Nano*, 2009, **3**, 2367.
22 D. B. Shinde and V. K. Pillai, *Chem. Eur. J.*, 2012, **18**, 12522.
23 B. L. Li, L. X. Chen, H. L. Zou, J. L. Lei, H. Q. Luo and N. B. Li, *Nanoscale*, 2014, **6**, 9831.
24 L. Bao, Z.-L. Zhang, Z.-Q. Tian, L. Zhang, C. Liu, Y. Lin, B. Qi and D.-W. Pang, *Adv. Mater*., 2011, **23**, 5801.
25 N. Liu, P. Kim, J. H. Kim, J. H. Ye, S. Kim and C. J. Lee, *ACS Nano*, 2014, **8**, 6902.
26 X. You, N. Liu, C. J. Lee and J. J. Pak, *MATER LETT*, 2014, **121**, 31.
27 Y.-P. Sun, B. Zhou, Y. Lin, W. Wang, K. A. S. Fernando, P. Pathak, M. J. Meziani, B. A. Harruff, X. Wang, H. Wang, P. G. Luo, H. Yang, M. E. Kose, B. Chen, L. M. Veca and S.-Y. Xie, *J. Am. Chem. Soc*., 2006, **128**, 7756.
28 A. Splendiani, L. Sun, Y. Zhang, T. Li, J. Kim, C.-Y. Chim, G. Galli and F. Wang, *Nano Lett.*, 2010, **10**, 1271.
29 T. Wang, L. Liu, Z. Zhu, P. Papakonstantinou, J. Hu, H. Liu and M. Li, *Energy Environ. Sci*, 2013, **6**, 625.
30 X.-J. Lv, G.-W. She, S.-X. Zhou and Y.-M. Li, *RSC Adv*., 2013, **3**, 21231.
31 D. Voiry, M. Salehi, R. Silva, T. Fujita, M. Chen, T. Asefa, V. B. Shenoy, G. Eda and M. Chhowalla, *Nano Lett.*, 2013, **13**, 6222.
32 W. Jaegermann and D. Schmeisser, *Surf. Sci*., 1986, **165**, 143.
33 Z. Wu, B. Fang, Z. Wang, C. Wang, Z. Liu, F. Liu, W. Wang, A. Alfantazi, D. Wang and D. P. Wilkinson, *ACS Catal*., 2013, **3**, 2101.
34 D. Gopalakrishnan, D. Damien and M. M. Shaijumon, *ACS Nano*, 2014, **8**, 5297.
35 V. Stengl and J. Henych, *Nanoscale*, 2013, **5**, 3387.
36 J. P. Wilcoxon, P. P. Newcomer and G. A. Samara, *J. Appl. Phys*., 1997, **81**, 7934.
37 J. E. Riggs, Z. Guo, D. L. Carroll and Y.-P. Sun, *J. Am. Chem. Soc*., 2000, **122**, 5879.
38 W. L. Wilson, P. F. Szajowski and L. E. Brus, *Science*, 1993, **262**, 1242.
39 J. Peng, W. Gao, B. K. Gupta, Z. Liu, R. Romero-Aburto, L. Ge, L. Song, L. B. Alemany, X. Zhan, G. Gao, S. A. Vithayathil, B. A. Kaipparettu, A. A. Marti, T. Hayashi, J.-J. Zhu and P. M. Ajayan, *Nano Lett.*, 2012, **12**, 844.
40 H. Li, X. He, Z. Kang, H. Huang, Y. Liu, J. Liu, S. Lian, C. H. A. Tsang, X. Yang and S.-T. Lee, *Angew. Chem. Int. Ed*., 2010, **49**, 4430.
41 Y.-M. Long, C.-H. Zhou, Z.-L. Zhang, Z.-Q. Tian, L. Bao, Y. Lin and D.-W. Pang, *J. Mater. Chem*., 2012, **22**, 5917.
42 H. Shi, R. Yan, S. Bertolazzi, J. Brivio, B. Gao, A. Kis, D. Jena, H. G. Xing and L. Huang, *ACS Nano*, 2012, **7**, 1072.
43 R. Doolen, R. Laitinen, F. Parsapour and D. F. Kelley, *J. Phys. Chem. B*, 1998, **102**, 3906.
44 M. A. Lukowski, A. S. Daniel, F. Meng, A. Forticaux, L. Li and S. Jin, *J. Am. Chem. Soc*., 2013, **135**, 10274.
45 J. Shi, D. Ma, G.-F. Han, Y. Zhang, Q. Ji, T. Gao, J. Sun, X. Song, C. Li, Y. Zhang, X.-Y. Lang, Y. Zhang and Z. Liu, *ACS Nano*, 2014, **8**, 10196
46 J. Xie, H. Zhang, S. Li, R. Wang, X. Sun, M. Zhou, J. Zhou, X. W. Lou and Y. Xie, *Adv. Mater*., 2013, **25**, 5807.
47 Y. Li, H. Wang, L. Xie, Y. Liang, G. Hong and H. Dai, *J. Am. Chem. Soc*., 2011, **133**, 7296.
48 A. B. Laursen, S. Kegnaes, S. Dahl and I. Chorkendorff, *Energy Environ. Sci*., 2012, **5**, 5577.